HHS Public Access

Author manuscript

Magn Reson Med. Author manuscript; available in PMC 2018 February 01.

Published in final edited form as:

Magn Reson Med. 2017 February ; 77(2): 841–847. doi:10.1002/mrm.26155.

Investigating Tumor Perfusion by Hyperpolarized ^{13}C MRI with Comparison to Conventional Gadolinium Contrast-Enhanced MRI and Pathology in Orthotopic Human GBM Xenografts

Ilwoo Park[1], **Cornelius von Morze**[1], **Janine M. Lupo**[1], **Jan H. Ardenkjaer-Larsen**[2,3], **Achuta Kadambi**[4], **Daniel B. Vigneron**[1], and **Sarah J. Nelson**[1,5]

[1]Surbeck Laboratory of Advanced Imaging, Department of Radiology and Biomedical Imaging, University of California, San Francisco, CA, United States

[2]GE Healthcare, Brøndby, Denmark

[3]Department of Electrical Engineering, Technical University of Denmark, Lyngby, Denmark

[4]Media Laboratory, Massachusetts Institute of Technology, Cambridge, MA

[5]Department of Bioengineering and Therapeutic Sciences, University of California, San Francisco, CA, United States

Abstract

Purpose—Dissolution dynamic nuclear polarization (DNP) enables the acquisition of ^{13}C magnetic resonance data with a high sensitivity. Recently, metabolically inactive hyperpolarized ^{13}C-labeled compounds have shown to be potentially useful for perfusion imaging. The purpose of this study was to validate hyperpolarized perfusion imaging methods by comparing with conventional Gadolinium (Gd)-based perfusion MRI techniques and pathology.

Methods—Dynamic ^{13}C data using metabolically inactive hyperpolarized bis-1,1-(hydroxymethyl)-[1-^{13}C]cyclopropane-d_8 (HMCP) were obtained from an orthotopic human Glioblastoma (GBM) model for the characterization of tumor perfusion and compared with standard Gd-based dynamic susceptibility contrast (DSC) MRI data and immunohistochemical analysis from resected brains.

Results—Distinct HMCP perfusion characteristics were observed within the GBM tumors compared to contra-lateral normal brain tissue. The perfusion parameters obtained from the hyperpolarized HMCP data in tumor were strongly correlated with normalized peak height measured from the DSC images. The results from immunohistochemical analysis supported these findings by showing a high level of vascular staining for tumor that exhibited high levels of hyperpolarized HMCP signal.

Conclusion—The results from this study have demonstrated that hyperpolarized HMCP data can be used as an indicator of tumor perfusion in an orthotopic xenograft model for GBM.

Corresponding author: Ilwoo Park, Email: ilwoo.park@ucsf.edu, 1700 4th Street, Box 2532, BH-303, University of California, San Francisco, CA 94158, USA.

Keywords

Dynamic nuclear polarization; hyperpolarized ^{13}C perfusion MRI; brain tumor; gadolinium dynamic susceptibility contrast imaging

Introduction

Glioblastoma multiforme (GBM) is the most malignant subtype of brain tumor, characterized by extreme heterogeneity, abnormal neovasculature and active angiogenesis. Gadolinium (Gd)-based perfusion imaging methods such as dynamic susceptibility contrast (DSC) magnetic resonance imaging (MRI) and dynamic contrast-enhanced (DCE) MRI have been used to measure GBM blood vessel volume and permeability, and have proven to be effective in assessing changes in tumor microvasculature and response to therapy (1,2).

Dissolution dynamic nuclear polarization (DNP) enables the acquisition of ^{13}C magnetic resonance spectroscopic imaging (MRSI) data with a huge gain in sensitivity over conventional ^{13}C MR methods (3). Recent studies using the hyperpolarized substrate [1-^{13}C]pyruvate have demonstrated the promise of this technique for examining *in vivo* tumor metabolism in brain tumors, including differentiating tumor from normal brain tissue as well as detecting early response to treatment in animal models of high-grade glioma (4-7).

While most of the studies using hyperpolarized ^{13}C compounds have focused on probing metabolically active substrates and their metabolic products, metabolically inactive hyperpolarized ^{13}C-labeled compounds can be used for angiography and perfusion imaging (8,9). Recent studies using metabolically inactive ^{13}C-labeled hyperpolarized compounds such as [^{13}C]urea and bis-1,1-(hydroxymethyl)-[1-^{13}C]cyclopropane-d_8 (HMCP) have demonstrated the feasibility of using these molecules as new perfusion MRI agents in preclinical cancer models (10,11). In contrast to standard Gd-based perfusion methods, the use of these hyperpolarized agents produces a signal that is directly proportional to concentration and background-free. While these prior studies showed the potential of applying metabolically inactive ^{13}C-labeled hyperpolarized compounds for perfusion imaging, this study was designed to directly compare the hyperpolarized perfusion imaging methods with the conventional Gd-based perfusion MRI techniques. Such a comparison will be beneficial in validating perfusion imaging with hyperpolarized agents and serve as preliminary data for the clinical translation of this technology. Dynamic ^{13}C imaging data using hyperpolarized HMCP were obtained from an orthotopic human GBM model for the characterization of tumor perfusion and compared with standard in vivo Gd-based DSC MRI data and immunohistochemical analysis of tissue samples from resected brains.

Materials and Methods

Animal Preparation

Seven six-week-old male athymic rats (rnu/rnu, homozygous, median weight=240g) that had been purchased from Harlan (Indianapolis, IN) were used for intracranial implantation of human GBM cells (G55 MG). The details of the cell culture and intracerebral implantation procedures have been described elsewhere (4,5). All rats underwent ^{13}C and ^{1}H imaging on

approximately the 18th day (range: 13th-23rd) after tumor cell implantation. Animal studies were approved by the Institutional Animal Care and Use Committee at our institution.

^{1}H and Hyperpolarized ^{13}C MRI

All animals were scanned on a 3 T clinical MRI system (GE Healthcare, Waukesha, WI, USA) with 40 mT/m, 150 mT/m/ms gradients, a multinuclear spectroscopy (MNS) hardware package, and a custom-designed ^{1}H/^{13}C rat coil. During each imaging session, rats were placed on a heated pad positioned inside the RF coil and in the MR scanner. Anesthesia was maintained with a constant delivery of isoflurane (1-2%). Prior to each ^{13}C imaging session, high-resolution T_2-weighted anatomical images were obtained in the axial plane using a fast spin-echo (FSE) sequence (TE/TR=60/4000 ms, 8 cm FOV, 192 × 192 matrix, 1.5 mm slice thickness and 8 NEX). For each ^{13}C experiment, a 50 μL aqueous sample of 7.2M HMCP (T_1=95 s ex vivo, 32 s in vivo at 3T) (8,11), 18 mM OX063 trityl radical (GE Healthcare, Oslo, Norway), and 1.5 mM Dotarem (Guerbet, Roissy, France) for polarization enhancement (12) was polarized using a HyperSense DNP polarizer (Oxford Instruments, Abingdon, UK) at 3.35T and 1.4K by irradiation with 94.1 GHz microwaves using methods described previously (3). After approximately 60 minutes of microwave irradiation, the mixture was rapidly dissolved in 5.6 mL phosphate-buffered saline, resulting in the agent having a concentration of 65 mM and pH ~7.5. The level of solid state polarization achieved in this study was similar to a previous study, which used the same sample formulation for HMCP (11). The liquid state polarization from the previous study, as measured by a low-field spectrometer, was 17-31%. A sample from the dissolved HMCP solution with volume of 2.7 mL was injected into the tail vein of the rat over a 12 s duration. At the start of the injection, dynamic images was acquired every second for 90s using a custom designed single-slice balanced steady state free precession (bSSFP) pulse sequence (TE/TR=6.5/13ms, flip angle=15°, matrix=32×24, resolution=2mm×2mm, slice thickness=5.4mm) (10). Following the acquisition of hyperpolarized HMCP data, T_1-weighted axial spin-echo images (TE/TR=10/700 ms, 8 cm FOV, 320 × 192 matrix, 1.2 mm slice thickness and 6 NEX) were obtained following an injection of 0.2 mmol/kg Magnevist® (Gd-DTPA) in order to define the extent of tumor. DSC images were obtained during a second intravenous administration of 0.2 mmol/kg Gd-DTPA that utilized a gradient echo, echo planar imaging sequence (EPI; TE/TR=28.2/500 ms, flip angle 35°, 8×8cm^2 in plane FOV and 40×40 matrix). The bolus of Gd-DPTA was injected manually into the tail vein at 15 s after the start of data acquisition, with a total of 150 time points obtained. The scan plane prescription including in-plane origin, spatial resolution (2×2 mm), and slice thickness (5.4 mm) were kept the same between hyperpolarized HMCP and DSC imaging, to allow a direct voxel-by-voxel comparison between the two methods. The first Gd-DTPA injection for the T_1-weighted imaging served as a preload method for the subsequent DSC acquisition, which has been shown to increase the accuracy and repeatability of DSC data post-processing and quantification (13,14).

Data Processing and Analysis

The methods used to process the ^{13}C HMCP data have been described previously (10,11). Dynamic HMCP images (Fig 1a) were obtained by 2D Fourier-transform of the raw HMCP data and regional magnitude HMCP signals were plotted over time (Fig 1c). Maximum peak

signal and area under the curve were normalized by their respective values from blood vessels, which were calculated as a mean from two vascular voxels with highest signal and compared between voxels containing tumor and contra-lateral normal tissue using a Wilcoxon sign-rank test. The time at maximum peak signal relative to the time at peak vascular signal was calculated and compared between tumor ($\Delta t_{max,tumor}$) and contra-lateral normal tissues ($\Delta t_{max,normal}$) (Fig 1c) using a Wilcoxon sign-rank test.

DSC images were processed using a previously described method (15,16). In short, the T2* signal time curve was converted to the change in relaxation rate (ΔR2*) and the peak height of this curve was calculated as the maximum ΔR2* signal (Fig 2b). Peak height values from voxels containing tumor were normalized by their respective values in normal brain tissue (nPH) and compared with both normalized maximum peak signal (nMP) and normalized area under the curve (nAUC) from the hyperpolarized HMCP data using a Pearson product-moment correlation test.

Immunohistochemistry

For immunohistochemical analysis of the vasculature, animals were euthanized after the imaging experiments. The brains were removed, fixed in phosphate-buffered 10% formalin, dehydrated by graded ethanols, and embedded in Paraplast Plus wax (McCormick Scientific, St. Louis, MO). Tissue sections were incubated with anti-α smooth muscle actin (α-SMA) antibody (Abcam, Cambridge, MA) to stain for vascular smooth muscle cells. The immunohistochemistry assays were performed on the Benchmark XT (Ventana Medical Systems, Mountain View, CA) using the UltraView detection system. The pixels with positive staining were counted from three randomly selected regions inside tumor with ×100 magnification using a threshold method in ImageJ (17).

Results

Representative data obtained with hyperpolarized HMCP imaging in GBM-bearing rats are shown in Figure 1. Dynamic ^{13}C imaging allowed for the consistent measurement of hyperpolarized HMCP signal in tumor, contra-lateral normal brain tissue, and blood vessels with high temporal (1s) and spatial ($2\times2\times5.4mm^3$) resolution (Fig 1a). The T_1-weighted post-Gd image in Figure 1b includes representative voxels for enhancing brain tumor (blue box), contra-lateral normal brain tissue (green box), and blood vessels outside the brain (red box). The time-resolved hyperpolarized ^{13}C imaging data were collected from throughout the rat brain for 90 sec, and the dynamic curves of tumor, contra-lateral normal brain tissue, and blood vessel were obtained as shown in Figure 1c. In normal brain tissue, relatively small amounts of hyperpolarized HMCP signal were observed, with high HMCP signal being detected in tumors. The SNR of the maximum peak signal and area under the curve were 22 ± 6 and 563 ± 152 (mean ± SD) for contra-lateral brain tissue, and 32 ± 10 and 974 ± 331 (mean ± SD) for tumor. The blood vessels displayed the highest HMCP signal with 88 ± 38 and 2118 ± 724 (mean ± SD) for the SNR of the maximum peak signal and area under the curve, respectively.

Representative DSC data acquired from GBM-bearing rats are shown in Figure 2. An axial T1 post-Gd image shows enhancing tumor and the corresponding grids for ΔR* curves (Fig

1a). The mean normalized peak height was 0.94 ± 0.22 (mean ± SD) for tumor, and ranged from 0.69 to 1.25.

Figure 3 compares HMCP signal characteristics between tumor, contra-lateral normal brain tissue, and blood vessel in seven tumor-bearing rats, showing differences that were statistically significant for various parameters. When normalized by the maximum peak signal from the reference blood vessel, the maximum peak signal (nMP) from tumor and contra-lateral normal tissue were 0.42 ± 0.28 and 0.26 ± 0.07 (mean ± SD), respectively. nMP for tumor was higher than nMP for normal tissue in all but one animal ($p<0.04$) (Fig 3a). The normalized area under the curve (nAUC) for tumor and normal tissue were 0.51 ± 0.32 and 0.26 ± 0.07 (mean ± SD), respectively. The nAUC for tumor was higher than nAUC for normal tissue in all animals ($p<0.02$) (Fig 3b). The hyperpolarized HMCP signal from contra-lateral brain tissue reached its maximum earlier than the signal from tumor and blood vessels (Fig 1c). The HMCP signal in contra-lateral normal tissue reached its maximum at 2.0 ± 1.8 s (mean ± SD) before its counterpart in blood vessels reached its maximum (Fig 3c). In contrast, tumor HMCP signal reached its maximum at 2.5 ± 2.6 s (mean ± SD) after its counterpart in blood vessels reached its maximum, suggesting that perfusion was delayed in tumor.

The tumor perfusion data obtained from hyperpolarized HMCP imaging was in excellent agreement with the conventional DSC imaging data. Figure 4 compares hyperpolarized HMCP dynamic data with the perfusion data that were acquired from seven GBM-bearing rats using conventional Gd-based DSC MRI . Figure 4a shows the relationship between nMP from HMCP signal from the hyperpolarized dynamic ^{13}C data and the nPH from DSC MRI in fifteen tumor voxels from seven rats. The total number of tumor voxels used for this analysis ranged from one to four per rat (Fig 4a). nMP values from hyperpolarized HMCP imaging were strongly correlated with nPH values from DSC imaging when all voxels were included in analysis ($p<0.01$, Fig 4a). This relationship also held for the mean values from each rat ($p<0.05$, Fig 4b). The nAUC was also strongly correlated with nPH when mean values from seven rats were compared between the two modalities ($p<0.02$, $r=0.8$, Fig 4c).

The immunohistochemical analysis of the vasculature confirmed the findings obtained from the hyperpolarized HMCP data. Figure 5 shows representative α-SMA stained slices. The rat shown in Figure 5a with a large amount of positive α-SMA staining (mean percent positive pixels=1.2 ± 0.54) in tumor vascular smooth muscle cells exhibited high HMCP parameters (mean nMP=0.5, mean nAU=0.6), while the rat shown in Figure 5b with relatively small amount of staining (mean percent positive pixels=0.055 ± 0.018) had smaller HMCP parameters (mean nMP=0.2, mean nAU=0.3).

Discussion

A specialized bSSFP pulse sequence that allowed for the dynamic imaging of hyperpolarized perfusion agent HMCP with a high spatial resolution (0.022 cm^3) and a high temporal resolution (1 s) for orthotopic GBM xenografts was used in this study. The long T_1 relaxation time (T_1=95 s ex vivo, 32 s in vivo at 3T) (8,11) and high polarization of HMCP enabled reliable assessment of perfusion from tumors, contra-lateral normal appearing brain,

and vasculature with high sensitivity (9,11). The results showed distinct HMCP perfusion within the GBM tumors, with higher maximum peak signal, area under the curve, and delayed maximum signal compared to contra-lateral brain tissue. The elevated hyperpolarized HMCP signal that was observed in tumors can most likely be attributed to the active angiogenesis that is typically present in high-grade gliomas (18-20).

Results from the hyperpolarized HMCP imaging were compared with data obtained using conventional Gd-based, DSC perfusion imaging in order to compare HMCP imaging with cerebral blood volume. The normalized maximum peak and area under the curve obtained from the hyperpolarized HMCP data in tumor were strongly correlated with normalized peak height measured from the DSC images (Fig 4). As the peak height from the ΔR2* curve in DSC images is proportional to the amount of cerebral blood volume (16), these hyperpolarized HMCP imaging parameters may represent an indirect estimate of blood volume, and provide a new method of estimating tumor perfusion with high sensitivity. The results from the immunohistochemical analysis further supported these findings by showing a high level of staining for tumor that exhibited high levels of hyperpolarized HMCP signal (Fig 5).

Recent studies using metabolically inactive hyperpolarized agents have demonstrated the utility of these agents for measuring tissue perfusion in vivo (10,11,21). These studies used [^{13}C]urea, [^{13}C]HMCP, and [^{13}C]t-butanol in mouse kidney, liver and healthy brain and have demonstrated the feasibility of monitoring permeability, perfusion, and transport in these tissues. However, hyperpolarized perfusion agents have not been applied to brain tumors or compared with gadolinium-based dynamic perfusion MRI methods. Our current study has demonstrated the potential of using the hyperpolarized perfusion agent HMCP for regional assessment of perfusion in orthotopic GBM xenografts and was validated by findings obtained using conventional Gd-enhanced DSC MRI and immunohistochemistry.

While we find this approach very promising, there are several limitations of this study. Although the proportionality of hyperpolarized HMCP signal to concentration is a theoretical advantage of HMCP perfusion imaging, signal dynamics are influenced by T1 decay and the possible variation of T1 relaxation between different tissues and across animals. The comparison of HMCP signal with Gd-enhanced DSC signal is complicated by variations in the volume, concentration and rate of injected compound between the two methods. In addition, it is very challenging to directly compare the two methods due to differences in kinetics and tissue perfusion of the two agents. Due to these possible complications, we simplified our quantification methods by normalizing the signal in tumor relative to the respective values from vasculature or normal brain tissue and aimed our study to demonstrate the correlation between the two perfusion methods. The results from our data have shown the distinct HMCP signal characteristics in different tissues (Fig 3) and the correlation between hyperpolarized HMCP and Gd-enhanced DSC perfusion parameters (Fig 4). The estimation of more quantitative measurements such as cerebral blood flow (CBF), cerebral blood volume (CBV) or mean transit time (MTT) may be possible; however, it is beyond the scope of this study.

Perfusion imaging using HMCP has several advantages over urea that has been used for hyperpolarized perfusion imaging in previous studies (10,11). HMCP has a much longer T1 compared to urea (95 s versus 47 s in solution at 3T) and crosses the blood-brain barrier (BBB) to a greater extent (21). In contrast, urea has a limited capacity to cross BBB due to a highly polar molecular structure and the corresponding low lipid bilayer permeability (22). While urea is an endogenous molecule and has low toxicity, the safety profile of HMCP has not been well studied and requires further investigation. No effects on heart rate or respiration were observed in our study.

In conclusion, this study has demonstrated that hyperpolarized HMCP data can be used as an indicator of tumor perfusion in an orthotopic xenograft model for GBM. The results from this study suggest that this technique may provide an alternative way to evaluate tumor perfusion for brain tumors that could be applied in patient studies.

Acknowledgments

The first author was supported by a basic research fellowship from the American Brain Tumor Association and a NCI training grant in translational brain tumor research (T32 CA151022). Support for the research studies came from NIH grants R01EB013427, P41EB013598, R00 EB012064, R21CA170148 and R01CA154915. CVM was supported by NIH grant K01DK099451.

References

1. Barrett T, Brechbiel M, Bernardo M, Choyke PL. MRI of tumor angiogenesis. Magn Reson Imaging. 2007; 26(2):235–49.
2. Essock-Burns E, Lupo JM, Cha S, Polley MY, Butowski NA, Chang SM, Nelson SJ. Assessment of perfusion MRI-derived parameters in evaluating and predicting response to antiangiogenic therapy in patients with newly diagnosed glioblastoma. Neuro Oncol. 2011; 13(1):119–31. [PubMed: 21036812]
3. Ardenkjaer-Larsen JH, Fridlund B, Gram A, Hansson G, Hansson L, Lerche MH, Servin R, Thaning M, Golman K. Increase in signal-to-noise ratio of > 10,000 times in liquid-state NMR. Proc Natl Acad Sci U S A. 2003; 100(18):10158–63. [PubMed: 12930897]
4. Park I, Larson PE, Zierhut ML, Hu S, Bok R, Ozawa T, Kurhanewicz J, Vigneron DB, Vandenberg SR, James CD, Nelson SJ. Hyperpolarized ^{13}C magnetic resonance metabolic imaging: application to brain tumors. Neuro Oncol. 2010; 12(2):133–44. [PubMed: 20150380]
5. Park I, Bok R, Ozawa T, Phillips JJ, James CD, Vigneron DB, Ronen SM, Nelson SJ. Detection of early response to temozolomide treatment in brain tumors using hyperpolarized ^{13}C MR metabolic imaging. J Magn Reson Imaging. 2011; 33(6):1284–90. [PubMed: 21590996]
6. Park I, Hu S, Bok R, Ozawa T, Ito M, Mukherjee J, Phillips JJ, James CD, Pieper RO, Ronen SM, Vigneron DB, Nelson SJ. Evaluation of heterogeneous metabolic profile in an orthotopic human glioblastoma xenograft model using compressed sensing hyperpolarized 3D (13)C magnetic resonance spectroscopic imaging. Magn Reson Med. 2013; 70(1):33–9. [PubMed: 22851374]
7. Park I, Mukherjee J, Ito M, Chaumeil MM, Jalbert LE, Gaensler K, Ronen SM, Nelson SJ, Pieper RO. Changes in pyruvate metabolism detected by magnetic resonance imaging are linked to DNA damage and serve as a sensor of temozolomide response in glioblastoma cells. Cancer Res. 2014; 1:74. (23):7115-24.
8. Svensson J, Månsson S, Johansson E, Petersson JS, Olsson LE. Hyperpolarized 13C MR angiography using trueFISP. Magn Reson Med. 2003; 50(2):256–62. [PubMed: 12876701]
9. Johansson E, Månsson S, Wirestam R, Svensson J, Petersson JS, Golman K, Ståhlberg F. Cerebral perfusion assessment by bolus tracking using hyperpolarized ^{13}C. Magnetic resonance in medicine. Magn Reson Med. 2004; 51(3):464–72. [PubMed: 15004786]

10. Von Morze C, Larson PE, Hu S, Keshari K, Wilson DM, Ardenkjaer-Larsen JH, Goga A, Bok R, Kurhanewicz J, Vigneron DB. Imaging of blood flow using hyperpolarized [(13)C]urea in preclinical cancer models. J Magn Reson Imaging. 2011; 33(3):692–7. [PubMed: 21563254]
11. Von Morze C, Larson PE, Hu S, Yoshihara HA, Bok RA, Goga A, Ardenkjaer-Larsen JH, Vigneron DB. Investigating tumor perfusion and metabolism using multiple hyperpolarized (13)C compounds: HP001, pyruvate and urea. Magn Reson Imaging. 2012; 30(3):305–11. [PubMed: 22169407]
12. Jóhannesson H1, Macholl S, Ardenkjaer-Larsen JH. Dynamic Nuclear Polarization of [1-13C]pyruvic acid at 4.6 tesla. J Magn Reson. 2009; 197(2):167–75. [PubMed: 19162518]
13. Hu LS, Baxter LC, Pinnaduwage DS, Paine TL, Karis JP, Feuerstein BG, Schmainda KM, Dueck AC, Debbins J, Smith KA, Nakaji P, Eschbacher JM, Coons SW, Heiserman JE. Optimized preload leakage-correction methods to improve the diagnostic accuracy of dynamic susceptibility-weighted contrast-enhanced perfusion MR imaging in posttreatment gliomas. AJNR Am J Neuroradiol. 2010; 31(1):40–8. [PubMed: 19749223]
14. Paulson ES, Schmainda KM. Comparison of dynamic susceptibility-weighted contrast-enhanced MR methods: recommendations for measuring relative cerebral blood volume in brain tumors. Radiology. 2008; 249(2):601–613. [PubMed: 18780827]
15. Lupo JM, Cha S, Chang SM, Nelson SJ. Dynamic susceptibility-weighted perfusion imaging of high-grade gliomas: characterization of spatial heterogeneity. AJNR Am J Neuroradiol. 2005; 26(6):1446–54. [PubMed: 15956514]
16. Cha S, Lu S, Johnson G, Knopp EA. Dynamic susceptibility contrast MR imaging: correlation of signal intensity changes with cerebral blood volume measurements. J Magn Reson Imaging. 2000; 11(2):114–9. [PubMed: 10713942]
17. Schneider CA, Rasband WS, Eliceiri KW. NIH Image to ImageJ: 25 years of image analysis. Nat Methods. 2012; 9(7):671–5. [PubMed: 22930834]
18. Amoroso A, Del Porto F, Di Monaco C, Manfredini P, Afeltra A. Vascular endothelial growth factor: a key mediator of neoangiogenesis: a review. Eur Rev Med Pharmacol Sci. 1997; 1:17–25. [PubMed: 9444794]
19. Brat DJ, Van Meir EG. Glomeruloid microvascular proliferation orchestrated by VPF/VEGF: a new world of angiogenesis research. Am J Pathol. 2001; 158:789–796. [PubMed: 11238026]
20. Wesseling P, Ruiter DJ, Burger PC. Angiogenesis in brain tumors; pathobiological and clinical aspects. J Neurooncol. 1997; 32:253–265. [PubMed: 9049887]
21. Von Morze C, Bok RA, Reed GD, Ardenkjaer-Larsen JH, Kurhanewicz J, Vigneron DB. Simultaneous multiagent hyperpolarized (13)C perfusion imaging. Magn Reson Med. 2014; 72(6): 1599–609. [PubMed: 24382698]
22. Levin VA. Relationship of octanol/water partition coefficient and molecular weight to rat brain capillary permeability. J Med Chem. 1980; 23:682–684. [PubMed: 7392035]

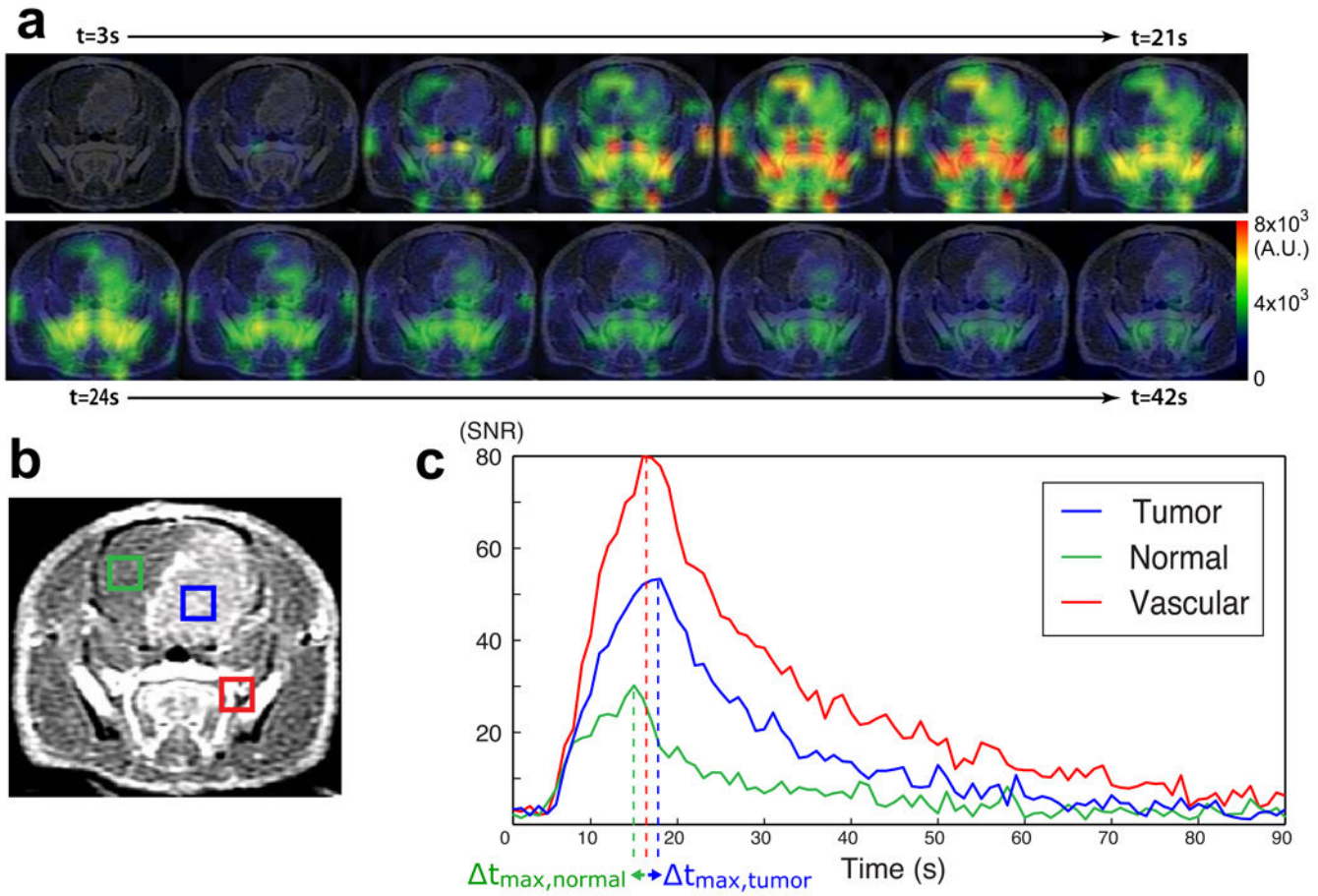

Figure 1.

Hyperpolarized HMCP data in a rat with orthotopic GBM. (a) The time course of HMCP signal change is shown in different regions of brain. (b) A representative axial T1 post-Gd image shows an enhancing lesion within the rat brain. The blue, green, and red voxels correspond to tumor, contra-lateral normal brain tissue, and blood vessel, respectively. (c) The plots of HMCP signal over time exhibit different perfusion characteristics for tumor, contra-lateral brain tissue, and blood vessel. Δt_{max} represents the time difference between peak tissue signal and peak vascular signal, for tumor and contra-lateral tissue.

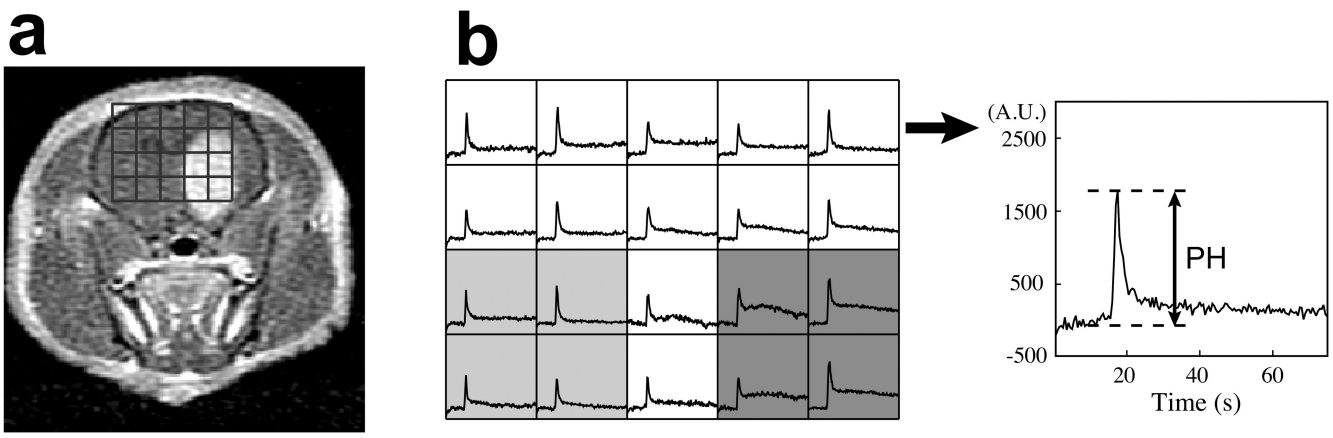

Figure 2.

Representative DSC data. (a) An axial T1 post-Gd image shows enhancing tumor. The grids indicate the spatial location of ΔR* curves in B. (b) In the corresponding ΔR* curves, peak height (PH) values in the tumor (dark grey) were normalized by the average PH from normal brain tissue (light grey voxels). The right panel in B shows an example of ΔR* signal evolution over the entire acquisition period (75 s).

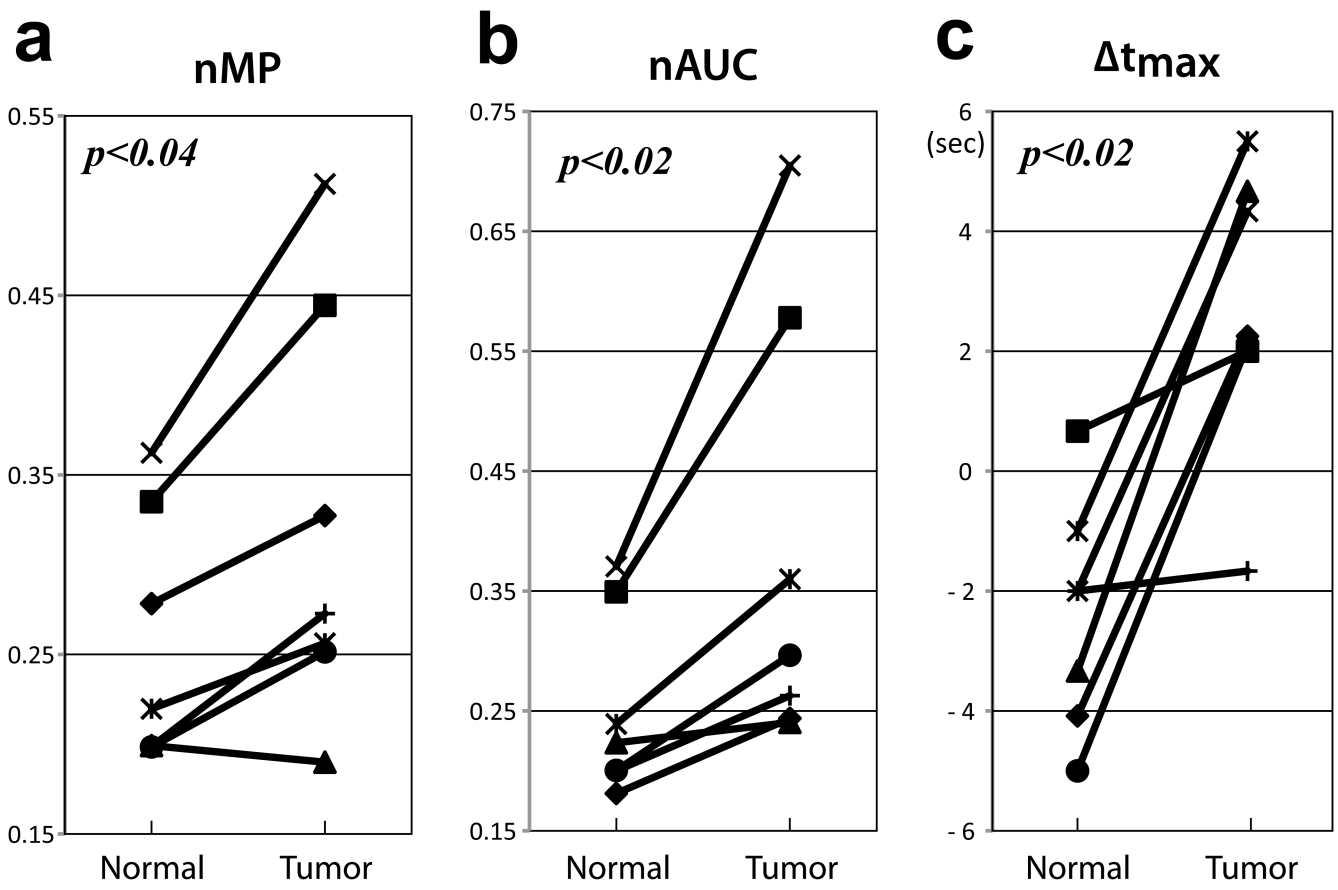

Figure 3.

A comparison of HP dynamic signal curve parameters from hyperpolarized HMCP data between tumor (Tumor) and contra-lateral brain tissue (Normal). The normalized maximum peak signal (nMP) (a), normalized area under the curve (nAUC) (b), and time at peak signal relative to time at peak vascular signal (c) showed significant differences between tumor and contra-lateral brain tissue.

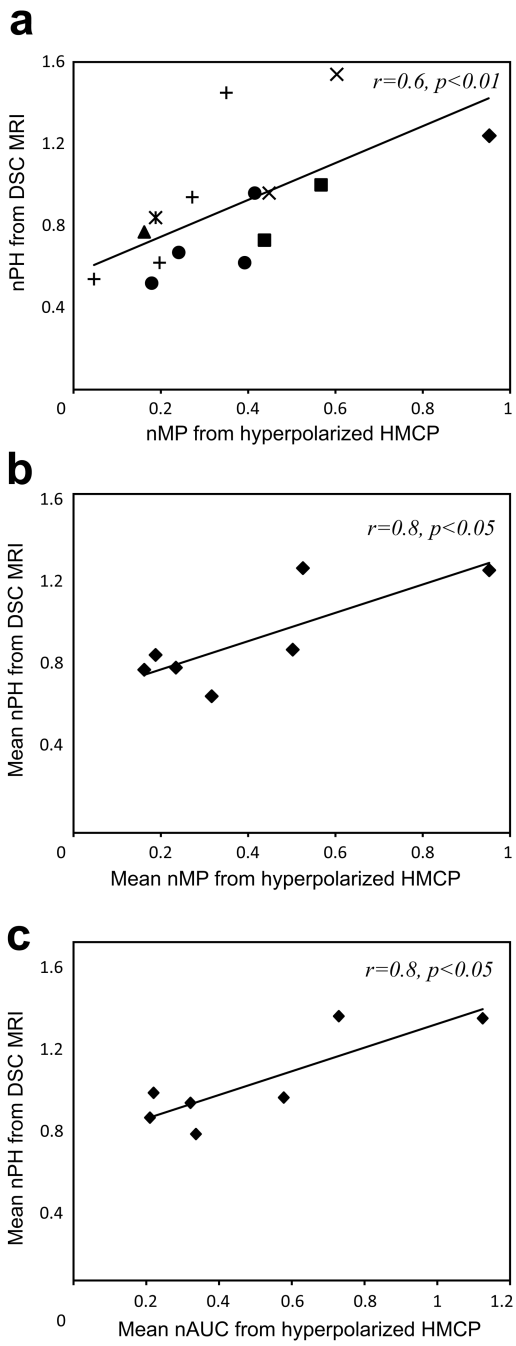

Figure 4.

Relationship between hyperpolarized ^{13}C HMCP and Gd-enhanced DSC MRI data from tumor voxels. (a) A significant correlation ($p<0.01$) between the normalized maximum peak signal (nMP) from hyperpolarized HMCP data and the normalized peak height (nPH) from DSC data was observed in all 15 tumor voxels from 7 rats. Individual shapes represent data from the same animal. When mean values were calculated for each animal, nMP (b) and normalized area under the curve (nAUC) (c) from hyperpolarized HMCP data strongly correlated with nPH from DSC data for all 7 rats.

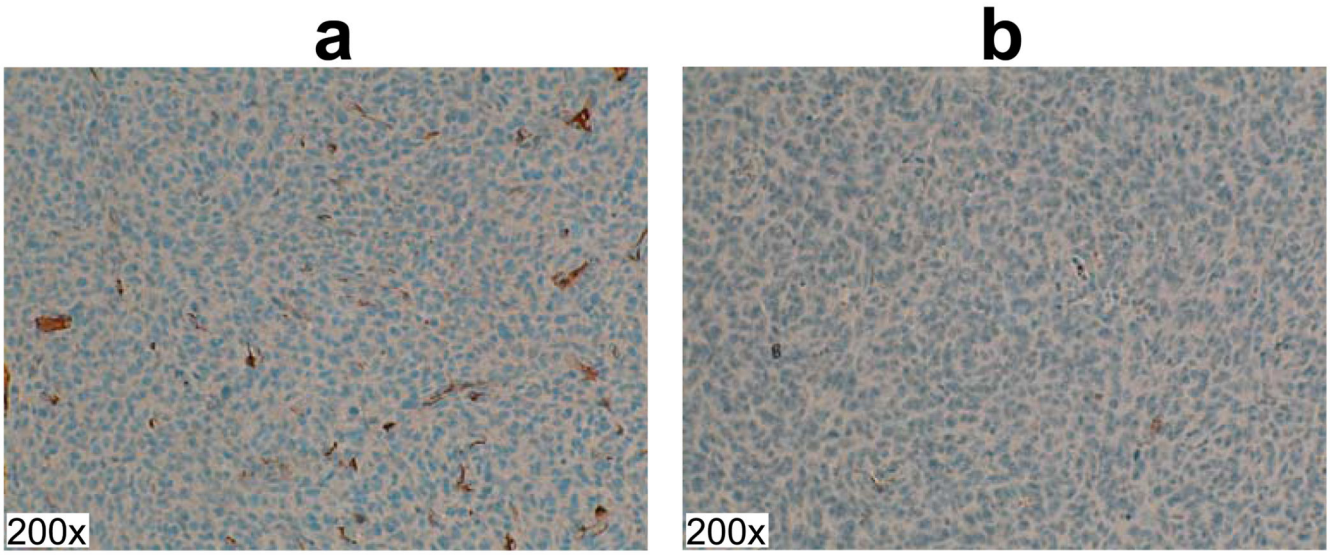

Figure 5.

Representative α smooth muscle actin slices for vascular staining. The red or dark brown regions represent stained smooth muscle cells in blood vessels. The animal with large amount of positive staining produced high perfusion values from hyperpolarized HMCP imaging (a, mean nMP=0.5, mean nAU=0.6), while the animal with small amount of positive staining produced small perfusion values hyperpolarized HMCP imaging (b, mean nMP=0.2, mean nAU=0.3). All images are at 200× magnification.